Scientific
Research
Publishing

A Complete DFT, TD-DFT and Non-Linear Optical Property Study on 6-Amino-2-Methylpyridine-3-Carbonitrile

Durai Sakthi[1], Madhu Prakasam[1,2], Annamalai Prakasam[3], Santhanam Sivakumar[4], Ponnusamy Munusamy Anbarasan[1,2*]

[1]Department of Physics, Periyar University, Salem, India
[2]Centre for Nanoscience and Nanotechnology, Periyar University, Salem, India
[3]Department of Physics, Thiruvalluvar Government Arts College, Rasipuram, Namakkal, India
[4]Department of Chemistry, E.R.K. Arts & College, Dharmapuri, India
Email: *profpmanbarasan@gmail.com

Abstract

The optimized geometric structure and photophysical properties of 6-Amino-2-methylpyridine-3-carbonitrile dye have been studied by using Density Functional Theory (DFT). The lowest singlet excited state geometry optimized using Time-Dependent Density Functional Theory (TD-DFT). On the basis of ground and excited state geometries, the absorption spectra have been calculated using the DFT and TD-DFT method in gas phase and acetonitrile medium. To understand the Non-Linear Optical properties of 6-Amino-2-methylpyridine-3-carbonitrile dye, we computed dipole moment (μ), electronic polarizability (α), and first hyperpolarizability (β_0) and second order hyperpolarizability (γ) using B3LYP density functional theory method in conjunction with 6-311++G(d) basis set.

1. Introduction

Since the work reported by O'Regan and Grätzel in 1991 [1], the metal-free organic sensitizers were investigated as a new generation solar cell of product materials in dye sensitized solar cells (DSSCs), due to their high conversion efficiencies of light-to-electricity, easy structural modifications and cost effective [2] [3] alternatives to conventional photovoltaic materials based on compound

semiconductors or inorganic silicon [4] [5]. As a key part of DSSCs, sensibilizers play a role in high power conversion efficiencies (PCEs). Simultaneously, most efficient organic sensibilizers like coumarin [6] [7], thiophene [8] [9], indoline [10] [11], triphenylamine [12] [13] have been tested in this D-π-A framework and good performances is observed. However, considerable progress has been made in the performance of DSSCs by experimental as well as theoretical methods; recently a rapid progress of organic dyes has been witnessed reaching close to 12.5%; that have been reported based on metal-free organic sensitizers [14]. Generally, the factors leading to the low photo-to-current conversion efficiency are the formation of serious intermolecular aggregation on the TiO_2 films as well as the charge recombination between the internal and external circuit current.

To have the experimentally observed photophysical properties of design of the 6-Amino-2-methylpyridine-3-carbonitrile dye with the desirable properties, theoretical investigations on the structure property relationship of these materials are essential. Quantum chemical methods play an important role to design and screen out efficient organic dyes reasonably, saving economical cost and synthesis efforts to investigate the relationship between electronic structures and the photophysical properties of the organic molecules [15] [16] [17]. The aim of the present work is to investigate the optimized geometries, polarizabilities and hyperpolarizabilities and the optical absorption properties of 6-Amino-2-methylpyridine-3-carbonitriles using DFT and TD-DFT.

In the present study, the optoelectronic properties of the designed molecules were studied using density functional theory (DFT) methods, calculation for the ground state and TD-DFT calculation for the excited state for the various rigid 6-Amino-2-methylpyridine-3-carbonitriles. Based on the optimized geometries we have calculated the absorption and emission spectra using the TD-DFT method with the B3LYP exchange correlation functional using 6-311++G(d,p) basis set. In this work, we computed dipole moment (μ), electronic Polarizability (α), mean first hyperpolarizability (β_0) and second order hyperpolarizability (γ).

2. Theory/Computational Method

The geometries of molecule were optimized using the Gaussian 09 suite of programs [18]. The ground state (S0) geometry of the 6-Amino-2-methylpyridine-3-carbonitrile dyes were optimized using DFT [19]. The B3LYP method combines Becke's three parameter exchange functional (B3) [20] with the nonlocal correlation functional by Lee, Yang and Parr (LYP) [21]. The basis set used for all atoms was 6-311++G(d,p). The vertical excitation energies and oscillator strengths were obtained for the lowest twenty singlet-singlet transitions at the optimized the ground state equilibrium geometries by using the Time-Dependent DFT (TD-DFT) at the same hybrid functional and basis set [22] [23]. All the calculations were carried out in solvent and gas medium using the Self-Consistent Reaction Field (SCRF) under the conductor like Polarizable Continuum Model (C-PCM) [24] [25]. In this work we have also calculated dipole moment (μ), electronic Polarizability (α), mean first Hyperpolarizability (β_0) and second Hyperpolarizability (γ) using B3LYP functional with the 6-311++G(d,p) basis

set. For completeness, we summarize the essential formulas used in our work, highlighting the quantities in which we are interested. Second-order non-linear optical properties of the 6-Amino-2-methylpyridine-3-carbonitrile chromophore. The components of β_0 are defined as the co-efficient in the Taylor series expansion of the energy in the external electric field. When the external electric field is weak and homogeneous, this expansion becomes.

$$E = E^0 - \mu_\alpha f_\alpha - \frac{1}{2\alpha_{\alpha\beta}F_\alpha F_\beta} - \frac{1}{6\beta_{\alpha\beta\gamma}F_\alpha F_\beta F_\gamma} \tag{1}$$

where E^0 is the energy of the unperturbed molecules, f_a is the field at the origin, μ_α, $\alpha_{\alpha\beta}$ and $\beta_{\alpha\beta\gamma}$ are the components of dipole moment, Polarizability and the first Hyperpolarizability, respectively [26].

The total static dipole moment μ is expressed by following equation

$$\mu_{tot} = \sqrt{\left(\mu_x^2 + \mu_y^2 + \mu_z^2\right)} \tag{2}$$

The isotropic Polarizability can be calculated from the trace of the polarization tensor,

$$\alpha_{tot} = \frac{1}{3}\left[\alpha_{xx} + \alpha_{yy} + \alpha_{zz}\right] \tag{3}$$

Anisotropy of the Polarizability $\Delta\alpha$ is expressed by

$$\Delta\alpha = \frac{1}{\sqrt{2}}\left[\left(\alpha_{xx} + \alpha_{yy}\right)^2 + \left(\alpha_{zz} + \alpha_{xx}\right)^2 + 6\alpha_{xx}^2\right] \tag{4}$$

The mean first Polarizability (β_0) is expressed by

$$\beta_0 = \left[\left(\beta_{xxx} + \beta_{xyy} + \beta_{xzz}\right)^2 + \left(\beta_{xxy} + \beta_{yyy} + \beta_{yzz}\right)^2 + \left(\beta_{xxz} + \beta_{zyy} + \beta_{zzz}\right)^2\right]^{1/2} \tag{5}$$

where β_{xxx}, β_{xyy}, β_{xzz}, β_{xxy}, β_{yyy}, β_{yzz}, β_{xxz}, β_{zyy} and β_{zzz} are the components of the first order hyperpolarizability tensor along the x, y, and z axes

The mean second Hyperpolarizability (γ) is expressed by

$$\gamma = \frac{1}{6}\left[\left(\gamma_{xxxx} + \gamma_{yyyy} + \gamma_{zzzz}\right) + 2\left(\gamma_{xxxx} + \gamma_{yyyy} + \gamma_{zzzz}\right)\right] \tag{6}$$

3. Results and Discussion

3.1. Geometric Structures in the Ground State

To understand the ground-state geometry of 6-Amino-2-methylpyridine-3-carbonitrile dye have been optimized at B3LYP/6-311++G(d) level of theory using C1 point group. As shown in **Figure 1** the bond length C1-C2 is increased from 1.395 to 1.398 Å. This change in the bond length indicates the charge transfer observed from pyridine ring to amino group. There are no changes observed in other bond length like C4-C5, C5-N10. The calculated bond length, bond length and dihedral angle as shown in **Table 1**.

The dihedral angle C2-C7-N8-C3-C1 for 6-Amino-2-methylpyridine-3-carbonitrile in acetonitrile solvent in S0 state is 179.89° while in S1 state it is 180° while this change in the indicating the charge transfer observed in 6-Amino-2-methylpyridine-3-carbonitrile.
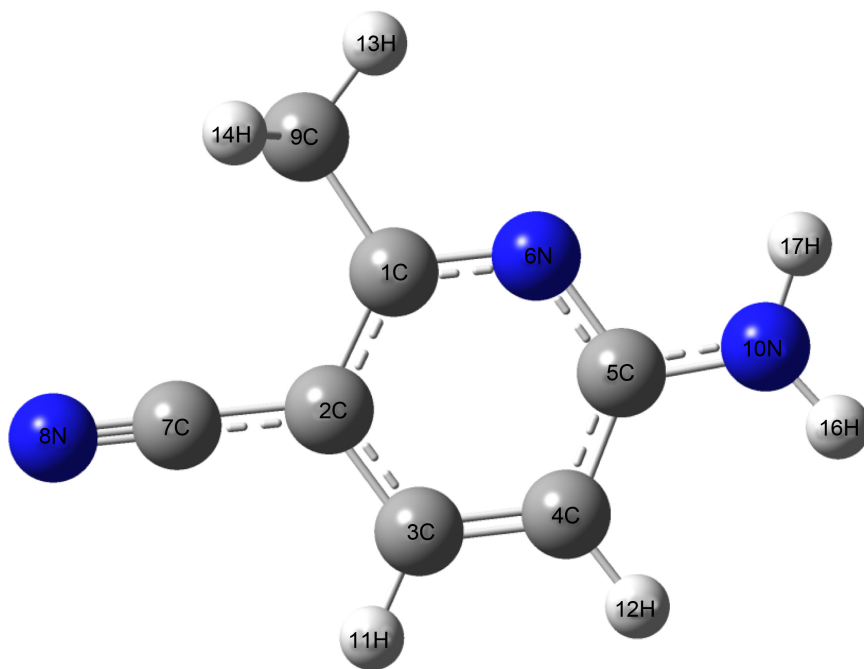
Figure 1. Optimized geometrical structure of dye 6-Amino 2-methylpyridine 3-carbonitrile.

3.2. Molecular Orbital Energies

Energy levels of the frontier molecular orbital's especially HOMO, LUMO, HOMO-1 and LUMO+1 as well as their spatial distributions are important parameters for determining the optoelectronic properties. The density plot of the HOMO and LUMO of 6-Amino-2-methylpyridine-3-carbonitrile is calculated at B3LYP/6-311++G(d) level of theory and are shown in **Figure 2**.

The orbital diagrams are plotted with the contour value of 0.02 a.u. The HOMO and LUMO plot of the studied 6-Amino-2-methylpyridine-3-carbonitrile molecules have the typical π molecular orbital characteristics. The HOMO (H)-LUMO (L) energy gap of 6-Amino-2-methylpyridine-3-carbonitriles is found in the range of 5.08 to 4.84 eV in acetonitrile medium. The lowest energy gap is observed for 6-Amino-2-methylpyridine-3-carbonitrile.

3.3. Electronic Absorption Spectra

The calculated vertical excitation spectra associated with their oscillator strength, composition, and assignments of 6-Amino-2-methylpyridine-3-carbonitrile dye in acetonitrile solvent is shown in **Table 2**. The theoretical λ_{max} reported in the following corresponds to the first singlet-singlet excited states with dipole allowed transition (*i.e.*, oscillator strength *f* is > 0) from the excited state. The absorption spectra for all the dyes are mainly due to the electronic transition from the HOMO to the LUMO. The calculated absorption wavelength is 398 nm for HOMO → LUMO transition. The absorption spectra for the 6-Amino-2-methylpyridine-3-carbonitriles in acetonitrile solvent computed at TD-B3LYP/6-311++G(d,p) level of theory are shown in **Figure 3**.

Table 1. Bond lengths (in Angstrom) bond angles (in degree) and dihedral angles (in degree) of the dye 6-Amino 2-methylpyridine 3-carbonitrile.

Parameters	HF/6-311++G(dp)	B3LYP/6-311++G(dp)
	Bond length (Å)	
C1-C2	1.3974	1.3935
C1-N6	1.331	1.3234
C1-C9	1.499	1.5077
C2-C3	1.3984	1.3955
C2-C7	1.4272	1.42
C3-C4	1.3704	1.3682
C3-H11	1.0701	1.0715
C4-C5	1.4026	1.401
C4-H12	1.0687	1.0695
C5-N6	1.3377	1.3343
C5-N10	1.3557	1.3504
C7-N8	1.1443	1.1417
C9-H13	1.0758	1.079
C9-H14	1.082	1.0843
C9-H15	1.082	1.0842
N10-H16	0.9865	0.9943
N10-H17	0.9878	0.9965
	Bond Angle (°)	
C2-C1-N6	120.9846	121.4585
C2-C1-C9	122.2144	121.0055
N6-C1-C9	116.801	117.5359
C1-C2-C3	118.3111	117.9168
C1-C2-C7	121.1808	121.485
C3-C2-C7	120.5081	120.5982
C2-C3-C4	120.3455	120.3895
C2-C3-H11	119.5153	119.466
C4-C3-H11	120.1392	120.1445
C3-C4-C5	117.9923	118.1306
C3-C4-H12	121.3012	121.2394
C5-C4-H12	120.7065	120.63
C4-C5-N6	121.5831	121.2692
C4-C5-N10	122.1604	122.3014
N6-C5-N10	116.2565	116.4294
C1-N6-C5	120.7834	120.8354
C1-C9-H13	109.2339	108.8366
C1-C9-H14	111.0716	110.5698
C1-C9-H15	111.0808	110.5917
H13-C9-H14	109.043	109.4568

Continued

H13-C9-H15	109.0508	109.4813
H14-C9-H15	107.3067	107.8869
C5-N10-C16	122.1444	122.4677
C5-N10-H17	118.421	118.0046
H16-N10-H17	119.4346	119.5278
Dihedral Angle (°)		
C2-C7-N8-C3-C1	179.8961	179.9429
C2-C7-N8-C3-C2	179.9985	179.9221
N6-C1-C2-C3	0.0015	−0.0285
N6-C1-C2-C7	179.9976	180.0041
C9-C1-C2-C3	−179.994	−180.0007
C9-C1-C2-C7	0.0023	0.032
C2-C1-N6-C5	−0.0011	0.0256
C9-C1-N6-C5	179.9944	179.9987
C2-C1-C9-H13	−179.903	−179.8984
C2-C1-C9-H14	59.7817	59.841
C2-C1-C9-H15	−59.5718	−59.5942
N6-C1-C9-H13	0.1017	0.1283
N6-C1-C9-H14	−120.214	−120.1322
N6-C1-C9-H15	120.4327	120.4326
C1-C2-C3-C4	−0.0017	0.0141
C1-C2-C3-H11	−180	−180.0304
C7-C2-C3-C4	−179.998	−180.0183
C7-C2-C3-H11	0.0038	−0.0628
C2-C3-C4-C5	0.0016	0.0024
C2-C3-C4-H12	−179.998	−180.0489
H11-C3-C4-C5	−180	180.0473
H11-C3-C4-H12	−0.0001	−0.0041
C3-C4-C5-N6	−0.0012	−0.0062
C3-C4-C5-N10	−180	179.9967
H12-C4-C5-N6	179.9987	180.0448
H12-C4-C5-N10	−0.0004	0.0477
C4-C5-N6-C1	0.001	−0.0079
N10-C5-N6-C1	−180	−180.0106
C4-C5-N10-H16	0.0002	−0.0014
C4-C5-C10-H17	180	−179.9848
N6-C5-N10-H16	−179.999	180.0014
N6-C5-N10-H17	0.0008	0.0179
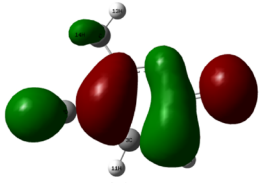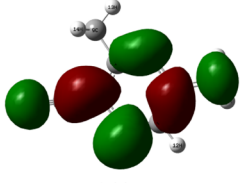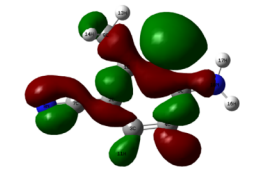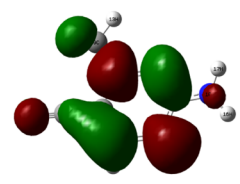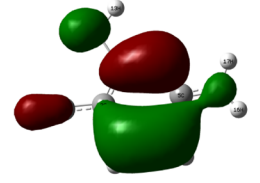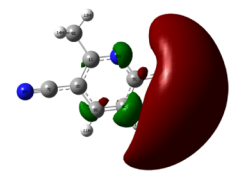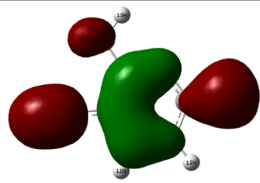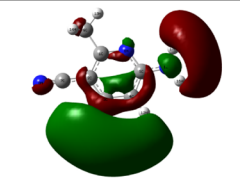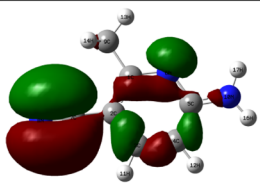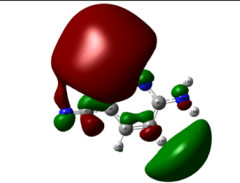
Table 2. Calculated maximum absorption wavelengths λmax/nm Oscillator strengths (f) and the corresponding electronic transitions assignment for Solvent (Acetonitrile) at TD-B3LYP/6-311++G(dp) level theory of the 6-Amino 2-methylpyridine 3-carbonitrile.

No	Wavelength (nm)	Osc Strength	Major Contributions
1	398.9423	0.0576	HOMO- > LUMO (89%)
2	359.5912	0.4328	HOMO- > L + 1 (90%)
3	342.0037	0.0077	H − 1- > LUMO (81%) H − 1- > L + 1 (12%)
4	329.2422	0.0087	H − 1- > LUMO (13%) H − 1- > L + 1 (80%)
5	312.3439	0.0003	HOMO- > L + 2 (96%)
6	306.199	0.035	H − 3- > LUMO (42%) H − 2- > L + 1 (46%)
7	288.6481	0.3546	H − 2- > LUMO (61%) H − 2- > L + 1 (20%)
8	284.4441	0.0698	H-3- > L + 1 (85%)
9	281.9939	0.2539	H − 3- > LUMO (51%) H − 2- > LUMO (16%) H − 2- > L + 1 (23%)
10	275.4771	0.0002	HOMO- > L + 4 (96%)
11	271.5819	0.0002	H − 4- > LUMO (17%) H − 4- > L + 1 (75%)
12	268.1518	0.064	H − 1- > L + 2 (15%) HOMO- > L + 3 (75%)
13	265.8529	0.007	H − 4- > LUMO (70%) H − 4- > L + 1 (15%)
14	263.4457	0.1227	H − 1- > L + 2 (66%) HOMO- > L + 3 (15%)
15	261.7863	0.0019	HOMO- > L + 5 (94%)
16	161.2372	0.0014	H − 3- > L + 2 (47%) H − 2- > L + 2 (43%)
17	155.4825	0.0315	H − 3- > L + 2 (39%) H − 2- > L + 2 (52%)
18	153.921	0.0109	H − 5- > LUMO (67%) H − 5- > L + 1 (20%)
19	152.3961	0.0098	H − 5- > LUMO (14%) H − 5- > L + 1 (68%)
20	152.1361	0.0193	H − 7- > LUMO (13%) H − 6- > LUMO (67%)

3.4. IR and Raman Frequencies

Figure 4 and **Figure 5** show the calculated IR and Raman spectra of 6-Amino-2-Methylpyridine 3-carbonitrile. Simulations of calculated IR and Raman spectra have been plotted using pure Lorentzian band shape with a bandwidth (FWHM) of 10 cm^{-1}. These calculations were done by using HF/6-311++G(d,p) and B3LYP/6-311++G(d,p). A corrective vibrational scaling factor of 0.9613 [27] [28] for B3LYP calculated frequencies and 0.8982 [29] [30] for HF calculated frequencies were applied to account the anharmonicity. **Table 3** presents the main features of HF/6-311++G(d,p) and B3LYP/6-311++G(d,p) calculated vibrational wavenumbers of 6-Amino-2-methylpyridine-3-carbonitrile. FT-IR spectra show six major vibrations viz., 828, 1367, 1647, 2321, 3622 and 3754 cm^{-1}. However, we observed 45 vibrations for 6-Amino-2-methylpyridine-3-carbonitrile but for clarity we consider only major vibrations. The peak at 828 cm^{-1} corresponds to C-H out of plane bending and 1367, 1647 cm^{-1} vibration is attributed to (C-N stretching + C-C stretching) and Ring symmetry deformation respectively. The peak observed around 2321 cm^{-1} can be assigned to C≡N stretching and C-N-N stretching in the nitrile group. The two peaks around 3622 and 3754

	HOMO	LUMO	
H	-6 47 eV	-1 39 eV	L
H-1	-7 74 eV	-1 2 eV	L+1
H-2	-8 28 eV	-0 42 eV	L+2
H-3	-8 83 eV	0 16 eV	L+3
H-4	-9 31 eV	0 32 eV	L+4

Figure 2. Isodensity plots (isodensity contour = 0 02 a. u) of the frontier orbitals of 6-Amino 2-methylpyridine 3-carbonitrile.
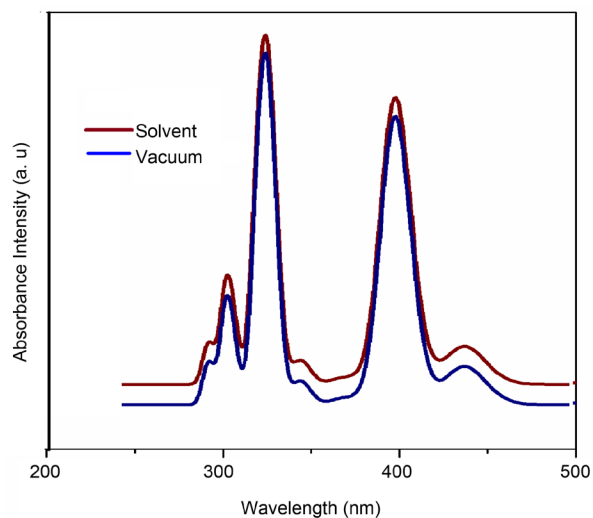
Figure 3. Experimental and calculated electronic absorption spectra of the dye 6-Amino 2-methylpyridine 3-carbonitrile.
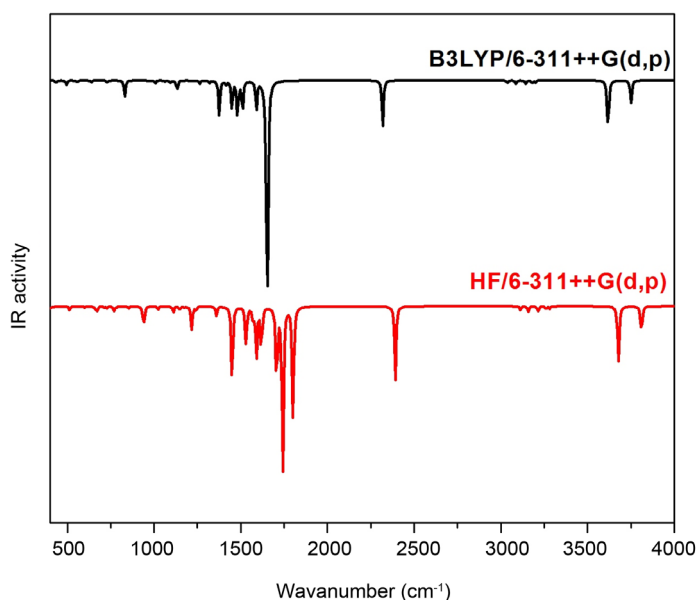
Figure 4. Observed and calculated FT-IR spectra of 6-Amino 2-methylpyridine 3-carbonitrile.
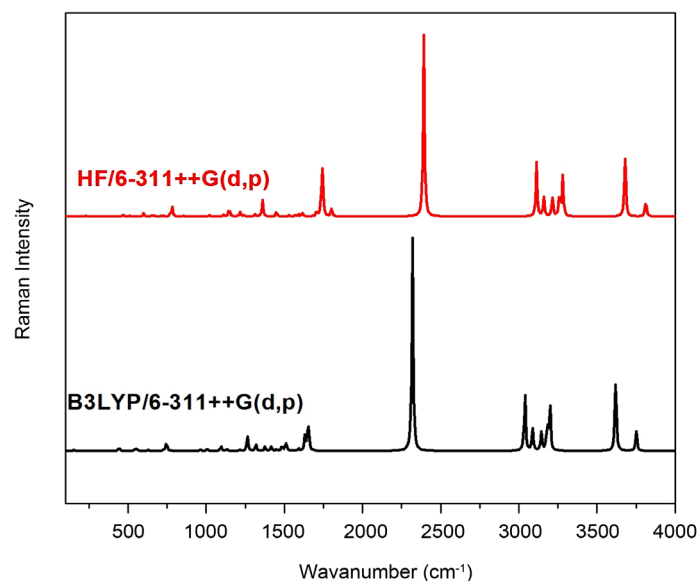
Figure 5. Observed and calculated FT-Raman spectra of 6-Amino 2-methylpyridine 3-carbonitrile.

cm^{-1} are attributed to CH-stretching, NH_2 asymmetry stretching and NH_2 symmetry stretching respectively. We observed six major bands in the Raman spectra of 6-Amino-2-methylpyridine-3-carbonitrile *i.e.*, 1656, 2316, 3033, 3198, 3612 and 3757 cm^{-1}. These bands are almost close observations with IR vibrational bands which confirm that molecule doesn't show any centro symmetry.

3.5. Nonlinear Optical (NLO) Properties

The computed the static dipole moment (μ), mean Polarizability (a_0), polarizability anisotropy (Δa), static first hyperpolarizability (β_0) and second hyperpola-

Table 3. Comparison of the observed (FT-IR and FT-Raman) and calculated vibrational frequencies of 6-Amino 2-methylpyridine 3-carbonitrile.

Vibrational Mode No	Species	Scaled Wavenumber (cm⁻¹)		IR Intensity	Raman active	Depolarisation Ratio	Reduced Mass	Force Constants	Assignments
		HF/ 6-311G(dp)	B3LYP/ 6-311G(dp)						
1	A"	137.2481	−230.6710	208.2942	0.1224	0.7500	1.2500	0.0392	C-C-N wagging
2	A'	226.6361	−42.0206	0.6154	0.3936	0.7500	1.0226	0.0011	C-C-N in plane bending
3	A'	247.6645	89.3826	0.6351	0.2869	0.7500	5.3105	0.0250	C-C-N wagging
4	A'	275.8585	147.0286	4.5510	3.2709	0.7367	6.9700	0.0888	C-C-N wagging
5	A'	307.8743	204.9280	2.1368	0.6190	0.7500	3.5819	0.0886	C-C-N wagging
6	A'	345.8385	244.5785	15.3787	0.0247	0.7500	6.1617	0.2172	C-C-N wagging
7	A"	356.8178	302.1178	2.6068	0.8094	0.2306	2.7821	0.1496	C N out-of-plane bending/C NH$_2$ out-of-plan bending C-C-N wagging
8	A"	461.4438	428.0724	4.4791	2.2073	0.4070	3.5812	0.3866	Ring torsion
9	A'	504.7169	434.3379	0.3144	0.6073	0.7499	3.0109	0.3347	Ring deformation
10	A'	506.5976	437.5242	1.2760	6.9229	0.4661	6.1649	0.6953	Ring deformation
11	A'	594.4737	488.5073	10.2675	0.2770	0.7500	1.1149	0.1568	Ring deformation
12	A'	645.6247	538.3456	0.7472	2.8741	0.7500	7.5074	1.2819	C-C-N in plane bending
13	A"	662.3708	548.7192	3.6029	7.7011	0.2418	5.1238	0.9090	C-C-N wagging + C-H wagging
14	A'	706.0825	623.3377	1.0183	2.5210	0.1731	6.2985	1.4419	C-C-N in plane bending
15	A'	721.8645	634.3828	3.1552	0.2450	0.7500	2.8630	0.6788	C-C-N in plane bending
16	A"	763.2812	725.1374	4.5887	3.6809	0.0820	5.9401	1.8403	C-C-N torsion + C-H wagging
17	A"	776.9993	740.0476	1.0834	24.6765	0.0675	5.7933	1.8694	C-C-N wagging + C-H wagging
18	A'	848.6116	764.0821	0.1320	0.9100	0.7500	3.9624	1.3630	C-H wagging
19	A"	934.3313	825.2243	35.8976	0.1022	0.7500	1.7438	0.6997	C-H wagging
20	A"	1016.0162	957.3793	1.9355	5.2794	0.0710	2.8161	1.5208	C-H wagging
21	A'	1105.1340	979.6123	0.7487	0.0901	0.7500	1.3218	0.7474	C-H wagging
22	A"	1122.5903	999.9477	6.2985	4.9994	0.1563	1.5463	0.9110	NH$_2$ twisting C-H wagging
23	A'	1141.9783	1055.0066	2.4242	0.0979	0.7500	1.5768	1.0340	C-H in plane bending
24	A'	1168.7041	1088.2283	5.4200	12.8089	0.3159	1.9768	1.3793	C-H in plane bending
25	A'	1211.5155	1126.9743	25.7020	6.0325	0.2407	1.8965	1.4191	C-H in plane bending
26	A'	1237.2237	1208.2387	1.2634	1.8696	0.6340	1.8834	1.6199	C-H in plane bending
27	A'	1306.7352	1258.3563	7.4179	40.5375	0.2081	2.5902	2.4165	C H in-plane bending C=C stretching
28	A'	1354.7238	1312.5856	5.2876	20.1536	0.2683	5.1622	5.2401	C NH$_2$ stretching C=C stretching

Continued

29	A'	1445.2228	1371.3791	79.7138	11.4304	0.1123	2.6404	2.9257	C=C stretching
30	A'	1525.2774	1410.8184	6.9224	11.3297	0.2495	1.3458	1.5782	C=C stretching + C-C-N stretching
31	A'	1566.6334	1444.3238	64.8143	3.6850	0.7130	2.4857	3.0552	C=C stretching
32	A'	1586.1876	1475.4126	70.9728	6.4055	0.3630	1.9148	2.4558	C=C stretching
33	A'	1609.1149	1481.8146	10.3112	7.4524	0.7500	1.0426	1.3489	C=C stretching
34	A'	1614.4543	1504.1393	78.6565	27.3271	0.3042	2.0077	2.6763	C=C stretching
35	A'	1702.6942	1586.0560	64.5878	5.9815	0.3840	4.4905	6.6555	C=C stretching
36	A'	1737.3665	1628.4756	8.6260	43.4980	0.6081	2.0770	3.2453	C=C stretching
37	A'	1797.7021	1647.9015	678.1377	97.3988	0.5025	2.5469	4.0749	N H asym stretch C=C stretching
38	A'	2388.6331	2315.7359	106.0110	627.7756	0.2980	12.6689	40.0284	C-N stretching
39	A'	3110.8977	3035.9037	5.1802	188.0729	0.0330	1.0382	5.6379	N H asym stretching C-N stretching
40	A'	3157.1658	3086.0360	7.0167	62.1457	0.7500	1.0994	6.1691	C-H stretching
41	A'	3212.4546	3141.5793	7.4582	53.3256	0.6698	1.1007	6.4003	CH$_3$ asym stretching
42	A'	3258.1776	3179.1493	6.1514	84.4806	0.5391	1.0887	6.4830	CH$_3$ asym Stretching
43	A'	3279.3012	3196.7648	4.9405	136.2234	0.1818	1.0963	6.6009	C-H stretching
44	A'	3677.4828	3617.9111	121.2816	243.8184	0.1583	1.0451	8.0602	C-H stretching
45	A'	3811.2136	3749.9172	54.7023	60.3263	0.7160	1.1055	9.1595	C-H inplane bending

rizability (γ) of 6-Amino-2-methylpyridine-3-carbonitrile molecule and which are gathered in Table 4 and Table 5 respectively. As can be seen, the mean polarizabilities of all 6-Amino-2-methylpyridine-3-carbonitrile are almost the same in gas phase as well as in solvent medium. But in case of polarizability anisotropy ($\Delta\alpha$), 6-Amino-2-methylpyridine-3-carbonitrile shows higher value (1.322×10^{-24} esu). Such a large value can be attributed to the lower compactness structure of this 6-Amino-2-methylpyridine-3-carbonitrile. The second-order nonlinear optical (NLO) properties originate from the non-centrosymmetric alignment of NLO. The first order Hyperpolarizability of 6-Amino-2-methylpyridine-3-carbonitrile calculated at B3LYP/6-311++G(d,p) level. The computed values for the first order Hyperpolarizability (β_0) for the 6-Amino-2-methylpyridine-3-carbonitrile were found to be greater than urea (3.71028×10^{-31}) by 3 times respectively using the B3LYP functional in the Solvent medium. This obtained large β_0 value confirms that there should be charge transfer characteristics of the first excited state. The calculated second order hyperpolarizability (γ) is 8.92×10^{-36} e.s.u. and second-order nonlinear optical property is found to be 13 times greater than urea (0.68×10^{-36}). This is because the ortho methyl group of the rigid 6-Amino-2-methylpyridine-3-carbonitrile core makes intramolecular hydrogen bonding with nitrogen and makes the structure planar. Due to the planarity, the intramolecular charge transfer (ICT) properties of the 6-Amino-2-methylpyridine-3-carbonitrile dyes get enhanced and result into an increase in β_0 value. A molecule with a large dipole moment and high molecular polarizability

Table 4. The calculated polarizability and Anisotropy of the polarizability components of 6-Amino 2-methylpyridine 3-carbonitrile.

*	α_{xx}	α_{xy}	α_{yy}	α_{xz}	α_{yz}	α_{zz}	α (esu)	$\Delta\alpha$ (esu)
DFT/6-311+G(dp)	−63.26	−7.0203	−53.472	0.0001	0.0000	−61.1477	8.786×10^{-24}	1.322×10^{-24}
HF/6-311G	−65.01	−7.5016	−53.534	0.0006	0.0002	−61.7588	8.906×10^{-24}	1.518×10^{-24}

Table 5. The calculated first order hyperpolarizability components of the 6-Amino 2-methylpyridine 3-carbonitrile.

| *	β_{xxx}	β_{xxy}	β_{xyy}	β_{yyy}	β_{xxz}	β_{xyz}	β_{yyz}	β_{xzz}	β_{yzz}	β_{zzz}	β_{ii} (esu)
DFT/6-311+G(dp)	147.4	13.71	8.358	−5.069	−0.002	−0.002	0.0007	−1.797	03.3174	0.003	1.334×10^{-30}
HF/6-311G	149.3	14.31	6.997	−4.871	−0.004	−0.002	0.0008	−1.9195	3.6094	0.003	1.338×10^{-30}

would be expected to exhibit high photoelectric conversion efficiency. The calculated dipole moment of the 6-Amino-2-methylpyridine-3-carbonitrile molecule charge direction shown in **Figure 6**. The dipole moment of the dye molecule in the gas phase and solvent medium is 6.06 and 6.41 Debye respectively. From these results, we can say that intramolecular charge transfer would be better facilitated by attachment of an electron-withdrawing amino group.

3.6. Mulliken Population Analysis

The natural population analysis of 6-Amino-2-methylpyridine-3-carbonitrile obtained by Mulliken [31] population analysis with B3LYP using basis set 6-311++G(d,p). The Mulliken charge calculated different levels and at same basis set listed in **Table 6**. The charge depending on basis set and are changed due to Polarizability. The C9 atom has more negative charge both HF/B3LYP/6-311++G(d,p), whereas the C2 atom has more positive charge than the other atoms see in **Figure 7**. The H and C atoms are electron acceptor and the charge transfer takes place from H to C. The N8 and C7 atoms by B3LYP/6-311++G-(d,p) methods are more positive than the other atoms due to electron accepting substitutions at that position in 6-Amino-2-methylpyridine-3-carbonitrile.

4. Conclusion

In the present work, DFT and HF calculations were used to optimize the geometry, structure and electronic properties of 6-Amino-2-methylpyridine-3-carbonitrile dye sensitizer. The strongest IR absorption for 6-Amino-2-methylpyridine-3-carbonitrile corresponds to the vibrational mode 31 near about 1444 cm⁻¹, which is the C=C stretching bonds. The next stronger IR absorption is attributed to vibrational mode 38 near about 2315 cm⁻¹, corresponding to C-N stretching bonds. The dye has a larger dipole moment in the excited state than in the ground state. The electron absorption spectra lie in visible and UV region. The polarizability and first order hyperpolarizability quantities of the 6-Amino-2-methylpyridine-3-carbonitrile molecule sensitizer are 8.786×10^{-24} and 11.334×10^{-30} respectively. The calculated polarizability anisotropy invariant of 2-Amino-6-Nitrobenzothiazole is 1.322×10^{-24} e.s.u. In summary, the reported results
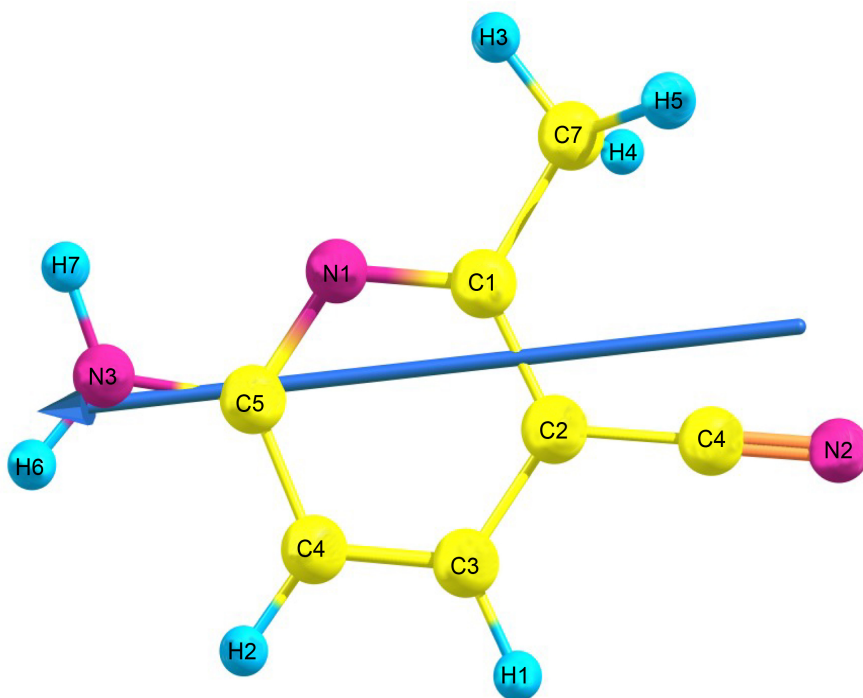
Figure 6. The Dipole moment of the 6-Amino 2-methylpyridine 3-carbonitrile.
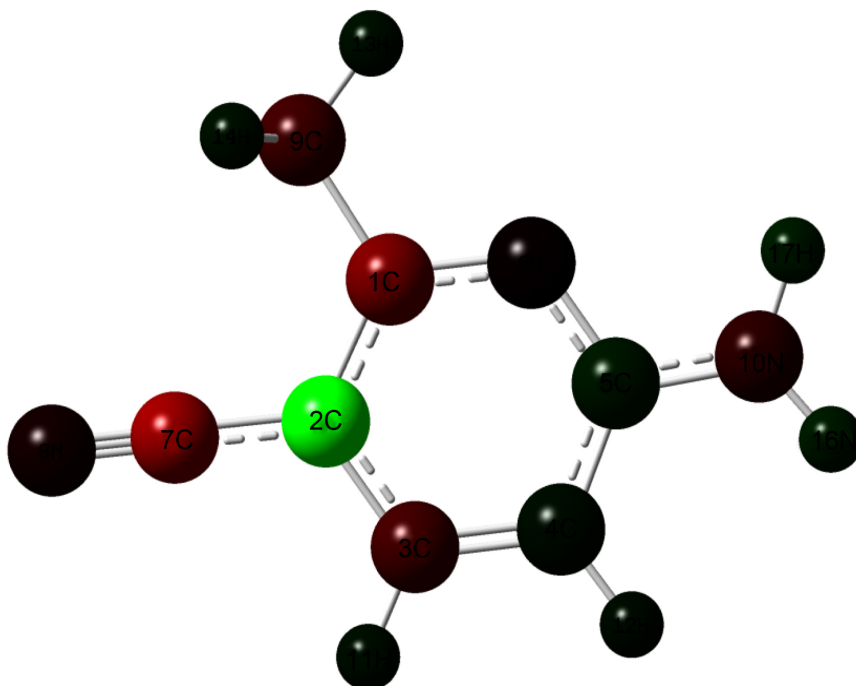
Figure 7. The calculated Mulliken atomic charge distribution of the 6-Amino 2-methylpyridine 3-carbonitrile.

illustrate that the 6-Amino-2-methylpyridine-3-carbonitrile molecules have good ability for the NLO properties. The above observations confirm that 6-Amino-2-methylpyridine-3-carbonitrile molecule as a dye sensitizer produces high photo to current conversion efficiency if we use it in practical DSSCs.

Table 6. The calculated Mulliken atomic charge distribution of the 6-Amino-2-methylpyridine-3-carbonitrile.

S No	Atom	Charge	
		HF/6311++G(dp)	B3LYP/6311++G(dp)
1	C	−1.1787	−1.1787
2	C	2.92013	2.920128
3	C	−0.6405	−0.6405
4	C	0.12759	0.12759
5	C	0.23118	0.231176
6	N	−0.06295	−0.06295
7	C	−1.46723	−1.46723
8	N	−0.19556	−0.19556
9	C	−0.60729	−0.60729
10	N	−0.42307	−0.42307
11	H	0.14109	0.141088
12	H	0.11938	0.119381
13	H	0.16211	0.162109
14	H	0.17105	0.171045
15	H	0.1709	0.170901
16	H	0.2591	0.259099
17	H	0.27278	0.272781

Acknowledgements

References

[1] O'Regan, B. and Grätzel, M. (1991) A Low-Cost, High-Efficiency Solar Cell Based on Dye-Sensitized Colloidal TiO_2 Films *Nature*, **353**, 737-740. https://doi.org/10.1038/353737a0

[2] Hagfeldt, A., Boschloo, G., Sun, L., Kloo, L. and Pettersson, H. (2010) Dye-Sensitized Solar Cells. *Chemical Reviews*, **110**, 6595-6663. https://doi.org/10.1021/cr900356p

[3] Ooyama, Y. and Harima, Y. (2009) Molecular Designs and Syntheses of Organic Dyes for Dye-Sensitized Solar Cells. *European Journal of Organic Chemistry*, 2903-2934. https://doi.org/10.1002/ejoc.200900236

[4] Hagfeldt, A. and Grätzel, M. (2000) *Accounts of Chemical Research*, **33**, 269-277. https://doi.org/10.1021/ar980112j

[5] Grätzel, M. (2001) Review Article Photoelectrochemical Cells. *Nature*, **414**, 338-344. https://doi.org/10.1038/35104607

[6] Wang, Z.-S., Cui, Y., Hara, K., Dan-Oh, Y., Kasada, C. and Shinpo, A. (2007) A High-Light-Harvesting-Efficiency Coumarin Dye for Stable Dye-Sensitized Solar Cells. *Advanced Materials*, **19**, 1138-1141. https://doi.org/10.1002/adma.200601020

[7] Koops, S.E., Barnes, P.R.F., O'Regan, B.C. and Durrant, J.R. (2010) Kinetic Competition in a Coumarin Dye-Sensitized Solar Cell: Injection and Recombination Limi-

tations upon Device Performance. *The Journal of Physical Chemistry C*, **114**, 8054-8061. https://doi.org/10.1021/jp910972x

[8] Yang, H.-Y., Yen, Y.-S., Hsu, Y.-C., Chou, H.-H. and Lin, J.-T. (2009) Organic Dyes Incorporating the Dithieno [3, 2-b: 2′, 3′ -d] Thiophene Moiety for Efficient Dye-Sensitized Solar Cells. *Organic letters*, **12**, 16-19. https://doi.org/10.1021/ol902327p

[9] Bai, Y., Zhang, J., Zhou, D., Wang, Y., Zhang, M. and Wang, P. (2011) Engineering Organic Sensitizers for Iodine-Free Dye-Sensitized Solar Cells: Red-Shifted Current Response Concomitant with Attenuated Charge Recombination. *Journal of the American Chemical Society*, **133**, 11442-11445. https://doi.org/10.1021/ja203708k

[10] Kuang, D., Uchida, S., Humphry-Baker, R., Zakeeruddin, S.M. and Grätzel, M. (2008) Organic Dye-Sensitized Ionic Liquid Based Solar Cells: Remarkable Enhancement in Performance through Molecular Design of Indoline Sensitizers. *Angewandte Chemie International Edition in English*, **47**, 1923-1927. https://doi.org/10.1002/anie.200705225

[11] Ito, S., Miura, H., Uchida, S., Takata, M., Sumioka, K., Liska, P., Comte, P., Péchy, P. and Grätzel, M. (2008) High-Conversion-Efficiency Organic Dye-Sensitized Solar Cells with a Novel Indoline Dye. *Chemical Communications*, No. 41, 5194-5196. https://doi.org/10.1039/b809093a

[12] Kozma, E., Concina, I., Braga, A., Borgese, L., Depero, L.E., Vomiero, A., Sberveglieri, G. and Catellani, M. (2011) Metal-Free Organic Sensitizers with a Sterically Hindered Thiophene Unit for Efficient Dye-Sensitized Solar Cells. *Journal of Materials Chemistry*, **21**, 13785-13798. https://doi.org/10.1039/c1jm12181b

[13] Sakong, C., Kim, H.J., Kim, S.H., Namgoong, J.W., Park, J.H., Ryu, J.H., Kim, B., Ko, M.J. and Kim, J.P. (2012) Synthesis and Applications of New Triphenylamine Dyes with Donor-Donor-(Bridge)-Acceptor Structure for Organic Dye-Sensitized Solar Cells. *New Journal of Chemistry*, **36**, 2025-2532. https://doi.org/10.1039/c2nj40374a

[14] Yao, Z., Zhang, M., Wu, H., Yang, L., Li, R. and Wang, P. (2015) Donor/Acceptor Indenoperylene Dye for Highly Efficient Organic Dye-Sensitized Solar Cells. *Journal of the American Chemical Society*, **137**, 3799-3802. https://doi.org/10.1021/jacs.5b01537

[15] Laurent, A.D., Adamo, C. and Jacquemin, D. (2014) Dye Chemistry with Time-Dependent Density Functional Theory. *Physical Chemistry Chemical Physics*, **16**, 14334-14356. https://doi.org/10.1039/C3CP55336A

[16] Laurent, A.D. and Jacquemin, D. (2013) TD-DFT Benchmarks: A Review. *International Journal of Quantum Chemistry*, **113**, 2019-2039. https://doi.org/10.1002/qua.24438

[17] Cramer, C.J. and Truhlar, D.G. (2009) Density Functional Theory for Transition Metals and Transition Metal Chemistry. *Physical Chemistry Chemical Physics*, **11**, 10757-10816. https://doi.org/10.1039/b907148b

[18] Frisch, M.J., Trucks, G.W., Schlegel, H.B., *et al.* (2009) Gaussian 09 Revision C 01 Gaussian 09 Revis B01. Gaussian Inc., Wallingford.

[19] Treutler, O. and Ahlrichs, R. (1995) Efficient Molecular Numerical Integration Schemes. *The Journal of Chemical Physics*, **102**, 346-354. https://doi.org/10.1063/1.469408

[20] Becke, A.D. (1993) Density-Functional Thermochemistry. III. The Role of Exact Exchange. *The Journal of Chemical Physics*, **98**, 5648-5652. https://doi.org/10.1063/1.464913

[21] Hehre, W.J., Radom, L., Schleyer, P.V. and Pople, J. (1986) *Ab Initio* Molecular Or-

bital Theory. Wiley, New York.

[22] Bauernschmitt, R. and Ahlrichs, R. (1996) Treatment of Electronic Excitations within the Adiabatic Approximation of Time Dependent Density Functional Theory. *Chemical Physics Letters*, **256**, 454-464.
https://doi.org/10.1016/0009-2614(96)00440-X

[23] Valeur, B. and Berberan-Santos, M.N. (2001) Molecular Fluorescence: Principles and Applications. Wiley, Weinheim.

[24] Tomasi, J., Mennucci, B. and Cammi, R. (2005) Quantum Mechanical Continuum Solvation Models. *Chemical Reviews*, **105**, 2999-3094.
https://doi.org/10.1021/cr9904009

[25] Cossi, M., Barone, V., Cammi, R. and Tomasi, J. (1996) *Ab Initio* Study of Solvated Molecules: A New Implementation of the Polarizable Continuum Model. *Chemical Physics Letters*, **255**, 327-335. https://doi.org/10.1016/0009-2614(96)00349-1

[26] Prakasam, M. and Anbarasan, P.M. (2016) Second Order Hyperpolarizability of Triphenylamine Based Organic Sensitizers: A First Principle Theoretical Study. *RSC Advances*, **6**, 75242-75250. https://doi.org/10.1039/C6RA11200E

[27] Singa, P., Boesch, S.E., Gu, C., Wheeler, R.A. and Willsom, A.K. (2004) Harmonic Vibrational Frequencies: Scaling Factors for HF, B3LYP, and MP2 Methods in Combination with Correlation Consistent Basis Sets. *The Journal of Physical Chemistry A*, **108**, 9213-9217. https://doi.org/10.1021/jp048233q

[28] Kabatc, J., Osmiałowski, B. and Paczkowski, J. (2006) The Experimental Studies on the Determination of the Ground and Excited State Dipole Moments of Some Hemicyanine Dyes. *Spectrochimica Acta Part A*, **63**, 524-531.
https://doi.org/10.1016/j.saa.2005.05.039

[29] Sun, Y., Chen, X., Sun, L., Guo, X. and Lu, W. (2003) Nanoring Structure and Optical Properties of Ga_8As_8. *Chemical Physics Letters*, **381**, 397-403.
https://doi.org/10.1016/j.cplett.2003.09.115

[30] Meic, Z. and Husten, G. (1978) Vibrational Studies of *trans*-Stilbenes—I. Infrared and Raman Spectra of *trans*-Stilbene and Deuterated *trans*-Stilbenes. *Spectrochimica Acta Part A*, **34**, 101-111. https://doi.org/10.1016/0584-8539(78)80193-7

[31] Mulliken, R.S. (1995) Electronic Population Analysis on LCAO-MO Molecular Wave Functions. I. *The Journal of Chemical Physics*, **23**, 1833-1840.
https://doi.org/10.1063/1.1740588